M&C 2017 - International Conference on Mathematics & Computational Methods Applied to Nuclear Science & Engineering, Jeju, Korea, April 16-20, 2017, on USB (2017)

CALENDF Probability Tables Advanced Self-shielding Factors Usage in the Inventory Code FISPACT-II

J.-Ch. Sublet, M. Fleming and M. R. Gilbert

United Kingdom Atomic Energy Authority, Culham Science Centre, Abingdon OX14 3DB, UK
jean-christophe.sublet@ukaea.uk, michael.fleming@ukaea.uk, mark.gilbert@ukaea.uk

Abstract - *The inventory code* FISPACT-II*, when connected to the nuclear data libraries TENDL-2015, ENDF/B-VII.1, JENDL-4.0u, CENDL-3.1 or JEFF-3.2, forms a simulation platform for modelling activation-transmutation processes and simulating radiation damage source terms. The system has added functionality to process extended nuclear data forms, including the ability to utilise probability table derived self-shielding factors to follow the correct multi-group reaction rates. In contrast to the traditional Bondarenko method, the probability table derived self-shielding factors extend to the unresolved resonance range for all channels and isotopic compositions, covering all nuclear plant types. Summaries of key findings are presented and comments are made on the processes put in place.*

I. INTRODUCTION

CALENDF [1, 2] is an R-matrix analysis and processing code with a variety of functionalities, including the generation of nuclear data forms for the inventory code FISPACT-II [3, 4] to address multi-group self-shielding. To achieve this, CALENDF is used to describe neutron cross section fluctuations corresponding to “cross section probability tables" based on Gauss quadrature and effective cross sections [5]. The full ENDF-6 point-wise cross section data and resonance parameters (resolved and unresolved) are used to generate unique probability table files which can be used by the inventory code FISPACT-II to calculate energy-dependent, dilution-specific self-shielding factors for all relevant reaction channels and energy ranges including both the resolved and unresolved resonance regions.

These data forms are been extensively used in the multi-physics data processing of the libraries needed by FISPACT-II. Also in the preparation of TENDL-2015, CALENDF has been used both to generate statistical resonances [6] for those many target nuclides with no, or only poor, resonance range experimental information, as well as to extract and assemble the probability tables from all evaluations of resolved and statistical resonance parameters.

Probability table data sets are supplied with FISPACT-II for each evaluation/library and temperature from the energy of 0.1 eV up to the end of the unresolved energy range of the evaluation. These are supplied in the same fine UKAEA-1102 group structure as the cross sections, as well as in the other supplied group structures. The same probability table forms are employed by the Monte Carlo code TRIPOLI [7, 8] in the unresolved energy range and by the fast deterministic code ERANOS [9, 10] with some restrictions in both resolved and unresolved resonance energy range.

CALENDF generates and manipulates these probability tables in various ways, including isotopic smearing, condensation, interpolation and order reduction. Effective cross sections and moments can then be extracted in the resolved and unresolved resonance ranges, while probability table self-shielding factors (ssf) are calculated for any competing channels and isotopic compositions. Note that the effective cross sections and moments derived in this way account not only for contributions to the self-shielding factors from all known channels and energies but also any isotopic mixture. There is some overlap of capabilities, regarding probability table forms with PREPRO multi-band or NJOY-purr, but the different processing codes are used as appropriate for the different forms of application data.

II. THEORY

Keywords in the FISPACT-II `input` file cause probability table sub-group data generated by CALENDF [2] to be used to model dilution effects in the computation of the collapsed effective cross sections. CALENDF provides data in five sets of macro-partial cross sections; the CALENDF set macro-`MT` numbers (cal-mt) are defined in Table I. The sum of these macro-partial cross sections gives the total cross section in each energy group over the resonance regions covered.

TABLE I. CALENDF macro-`MT` number.

cal-mt	Description	`MT` in set
2	elastic scattering	2
101	absorption (no outgoing neutron)	102 103 107
18	fission total	18
4	inelastic scattering (emitting one neutron)	4 11
15	multiple neutron production (excluding fission)	5 16 17 37

The data provided by CALENDF are effective cross-section σ and probability values P depending on four parameters,

$$\sigma(x,n) \equiv \sigma(p,g,x,n) \quad (1)$$

$$P(x,n) \equiv P(p,g,x,n)\,, \quad (2)$$

where
p = parent nuclide number,
g = energy group number,
x = macro-partial (or total) index, and
n = Gaussian quadrature index.

In the expressions below, we suppress the explicit display of dependence of cross section on the parent nuclide p and energy group g except in the formulae for dilution. The infinite dilution ($d = \infty$) cross section for a given parent, energy group and component is

$$\begin{aligned}\sigma(x, d = \infty) &= \frac{1}{E_{max} - E_{min}} \int_{E_{min}}^{E_{max}} \sigma(E)\, dE \\ &= \sum_{n=1}^{N} P(x, n)\sigma(x, n)\,. \end{aligned} \tag{3}$$

When a nuclide is a part of a homogenous mixture of nuclides, then the effective cross sections in the resonance regions are reduced, and are parameterised using the dilution cross section d [11, 12, 13, 2],

$$\sigma(x, d) = \frac{\sum_{n=1}^{N} P(x, n)\sigma(x, n)/(\sigma_t(n) + d)}{\sum_{n=1}^{N} P(x, n)/(\sigma_t(n) + d)}\,, \tag{4}$$

where the total cross section is given by the sum of the macro-partials,

$$\sigma_t(n) = \sum_{x=1}^{X} \sigma(x, n)\,. \tag{5}$$

The total cross section for nuclide p in energy group g at dilution d is given by

$$\sigma^{tot}(d) = \sum_{x=1}^{X} \sigma(x, d_p)\,. \tag{6}$$

The probability table data from CALENDF are used in conjunction with the 709 and 1102 group data in the TENDL library, as well as any other ENDF-6 formatted library. In the following discussion, we use the term 'library' or 'LIB' to refer to either the TENDL or alternative ENDF-6 forms as appropriate. The dilution computed using the CALENDF data is applied either as scaling factors to the library cross-section data or as replacements over the energy ranges for which the probability table data are available. This is selected by user input. If the CALENDF and library data were fully self-consistent, then the same self-shielding would be obtained for scaling and for replacement, but the treatment of elastic scattering cross section in certain evaluations could leads to some differences. For both the scaling or replacement approach, partial or total scaling may be selected by user input.

1. Scaling applied to library data:

Scaling is applied to the library data in one of two ways depending on user input. If the partial self-shielding scaling factor option is chosen, then the cross section for nuclide p in energy group g and for `MT` value y belonging to the macro-partial group x is scaled according to

$$\sigma^{new}(y, d) = \sigma^{LIB}(y)\left(\frac{\sigma(x, d)}{\sigma(x, d = \infty)}\right) \tag{7}$$

and for the total scaling factor

$$\sigma^{new}(y, d) = \sigma^{LIB}(y)\left(\frac{\sigma^{tot}(d)}{\sigma^{tot}(d = \infty)}\right)\,. \tag{8}$$

The dilution $d(p, g)$ for a given nuclide p and energy group g is computed using a weighted sum over all the nuclides, $q \in [1, Q]$ in the mixture. The fraction of nuclide q in the mixture is f_q. Nuclides in the mixture may or may not be included in the list of nuclides to which the self-shielding correction is to be applied. Nuclides to which self-shielding corrections are applied must be in the mixture list. The first approximation is given using the total cross sections from the cross-section library as

$$d^{(0)}(p, g) = \sum_{\substack{q=1 \\ p \neq q}}^{Q} \frac{f_q \sigma^{LIB-tot}(q, g)}{f_p}\,, \tag{9}$$

where

$$\sigma^{LIB-tot}(p, g) = \sum_{y} \sigma^{LIB}(p, g, y)\,. \tag{10}$$

Over the energy range for which the probability table data are available for those nuclides in the mixture for which self-shielding corrections are being applied, the approximation given by Eq. (9) is iteratively refined using

$$\begin{aligned} S^{(i)}(g) &= \sum_{q=1}^{Q} f_q \sigma^{LIB-tot}(q, g) \times \\ &\quad \left(\frac{\sigma^{tot}(q, g, d^{(i)}(q, g))}{\sigma^{tot}(q, g, \infty)}\right) \end{aligned} \tag{11}$$

$$\begin{aligned} d^{(i+1)}(p, g) &= \frac{S^{(i)}(g)}{f_p} - \sigma^{LIB-tot}(p, g) \times \\ &\quad \left(\frac{\sigma^{tot}(p, g, d^{(i)}(p, g))}{\sigma^{tot}(p, g, \infty)}\right)\,. \end{aligned} \tag{12}$$

2. Replacement of library data:

If there is only one reaction `MT` in the CALENDF macro-partial group, then the replacement formulae would be given by replacing the σ^{LIB} values in the above equations by the infinite dilution cross sections obtained from the CALENDF data. When there is more than one reaction in the macro-partial set, then the dilution effect has to be apportioned according to the LIB reaction cross sections.

If the partial self-shielding scaling factor option is chosen, then the cross section for nuclide p in energy group g and for `MT` value y belonging to the macro-partial group x is given by

$$\sigma^{new}(y, d_p) = \sigma(x, d_p)\left(\frac{\sigma^{LIB}(y)}{\sum_{y' \in x} \sigma^{LIB}(y')}\right) \tag{13}$$

and for the total scaling factor

$$\begin{aligned} \sigma^{new}(y, d_p) &= \sigma(x, \infty)\left(\frac{\sigma^{LIB}(y)}{\sum_{y' \in x} \sigma^{LIB}(y')}\right) \times \\ &\quad \left(\frac{\sigma^{tot}(d_p)}{\sigma^{tot}(\infty)}\right)\,. \end{aligned} \tag{14}$$

The initial values of the dilutions are given by Eqs (9) and (10) and the iterative refinements where CALENDF probability table data are available are given by

$$S^{(i)}(g) = \sum_{q=1}^{Q} f_q \sigma^{tot}(q,g,d^{(i)}(q,g)) \quad (15)$$

$$d^{(i+1)}(p,g) = \frac{S^{(i)}(g)}{f_p} - \sigma^{tot}(p,g,d_p^{(i)}) . \quad (16)$$

The set of nuclides for which the self-shielding correction is calculated and the set of nuclides included in the mixture for computing the dilution cross section is specified user input. User input also allows the values of dilution given by Eq. (12) or (16) to be overridden by user-supplied dilution values.

The default method of computing self-shielding using the probability table method is to use Eqs (9) and (10) for initial values, Eq. (13) for cross section and iterate dilution using Eqs (15) and (16). When the iteration is complete, the new collapsed cross sections are computed by applying the ssf to produce the effective cross sections. The effective self-shielding factor ssf for the collapsed cross section is given by

$$ssf(p,y) = \frac{\sigma^{new}(p,y)}{\sigma^{LIB}(p,y)} . \quad (17)$$

The self-shielding factors may be applied wherever probability table data are provided and can be used to correct specific sets of reaction rates for desired nuclides, for example the energy-dependent self-shielding factors applied to the ^{235}U neutron fission in a typical PWR spectrum and fresh fuel composition, which is shown in Fig. 1. These can be updated during irradiation, accommodating changes in both nuclide inventory and spectra to alter the dilutions and reaction rates, respectively.

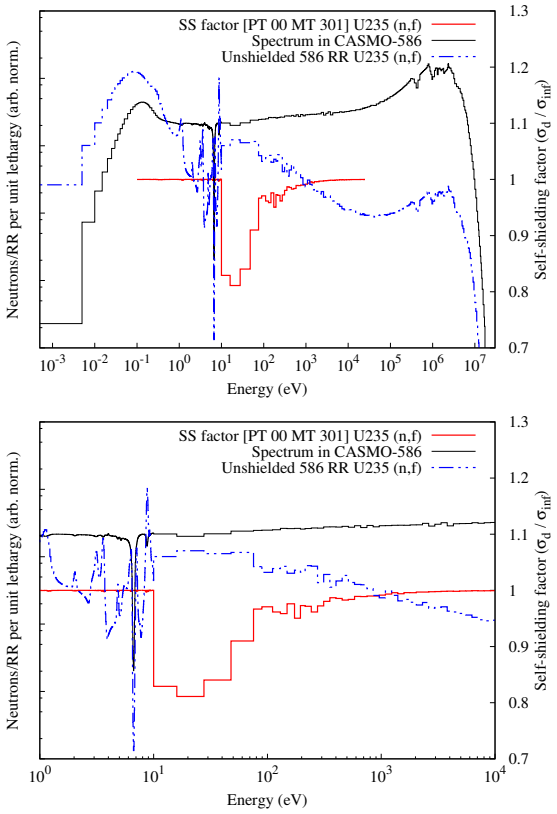

Fig. 1. Neutron spectrum, the unshielded ^{235}U(n, f) cross section and the energy-dependent probability table self-shielding factors calculated for the fresh fuel composition in FISPACT-II using ENDF/B-VII.1. Global and zoomed-in plots are provided.

III. APPLICATIONS

Cross section probability tables are the basic data of the multi-band (or sub-group) method and are used in many neutron transport codes with various implementations, as now in the inventory code FISPACT-II. Their usage has been proven most beneficial, particularly in fast energy applications, but also in epithermal and shielding applications. The resulting enhancements, when compared with a straightforward multi-group (see Fig. 2) calculation, are significant. While conserving the number of groups and without significant increase in simulation time, the discrete ordinate multi-band method allows improved accuracy in reactor, shielding and now inventory simulations. Group-wise reaction rate calculations benefit as well from such enhanced effective cross section representation data. Even point-wise Monte-Carlo calculations rely upon them, but of course only in the unresolved resonance range [14].

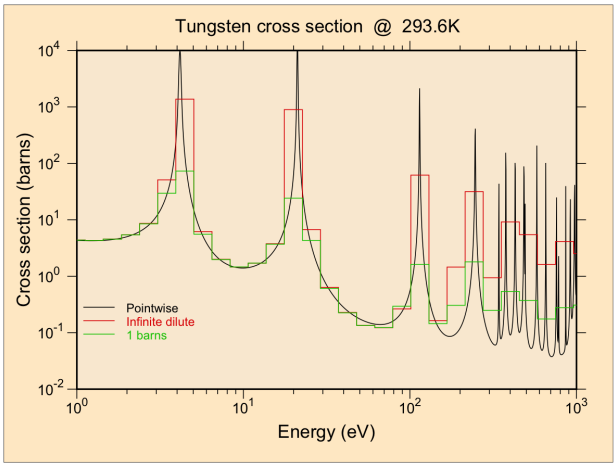

Fig. 2. Tungsten point-wise and multi-group total cross section, showing both the infinitely dilute and 1 barn effective multi-group cross sections.

IV. CROSS SECTION GROUP STRUCTURE

There are three standard group structures in the ENDF-6 format used for the TENDL, ENDF/B-VII.1, JENDL-4.0, CENDL-3.1 and JEFF-3.2 nuclear libraries. Data in these

structures can be read automatically into FISPACT-II and used to collapse with an incident particle spectrum in the corresponding structure.

Each possesses a fine energy grid, an increased upper energy bound of up to 1 GeV, and allow the addition of α and γ-induced reactions while permitting more precise modelling of reaction thresholds and the resolved and unresolved resonance ranges. These groups are the CCFE-162 (charged particles), CCFE 709 (TART-660 extension) and the UKAEA-1102 [4], an amalgamation of CASMO [15] thermal, TART [16] and UKAEA fast group structures.

The group structures for the UKAEA-1102 and its predecessors are shown in Fig. 3, depicted in equal energy bin width, lethargy and cumulative number of energy groups. These illustrate which energy ranges are targeted by each structure and will therefore give an accurate representation of the reaction rates.

The CCFE-162 (up to 200 MeV) structure was introduced for studies of charged-particle projectiles and γ-induced activation and transmutation. This structure includes all legacy ones known to the authors, because past limitations of computing resources are no longer a consideration justifying simpler energy structures. The CCFE (709 up to 200 MeV and 660 up to 30 MeV) group structures are extensions of the LLNL (616 up to 20 MeV) structure. They have 50 energy groups per energy decade, equally spaced in the logarithm of the energy between 10^{-5} eV and 10 MeV, 200 keV steps to 30 MeV and thereafter bins with appropriately chosen equally-spaced boundaries in energy up to 1 GeV. The UKAEA 1102-group structure is the culmination of extensions of the thermal fission CASMO5 (586) [15], the fast LLNL (616) and the fast CCFE (709) structures pushed to 1 GeV. Each specific feature of those three grids have been combined into one single structure: the UKAEA 1102-group structure depicted in Fig. 4.

The generation of reaction rates with multi-group convolution of binned fluxes with cross-sections has always been the subject of intense research in order to satisfy the specific requirements of one application at a time. Recent studies [17, 18] have demonstrated that the fine CCFE-709 and *a fortiori* the UKAEA-1102 group structure have been optimised to comprehensively cover most applications.

V. RESULTS AND ANALYSIS

In FISPACT-II the set of nuclides for which the self-shielding correction is calculated, and the set of nuclides included in the mixture for computing the dilution cross section, is a user-specified input. These can include any and all nuclides for which probability table is provided (2601 target nuclides for the TENDL-2015 neutron-induced data). User input also allows the values of dilution that have been calculated automatically to be overridden by user-supplied dilution values.

The user has multiple choices of method for computing self-shielding using the probability table method. When the iterative dilution calculation is complete, the new collapsed

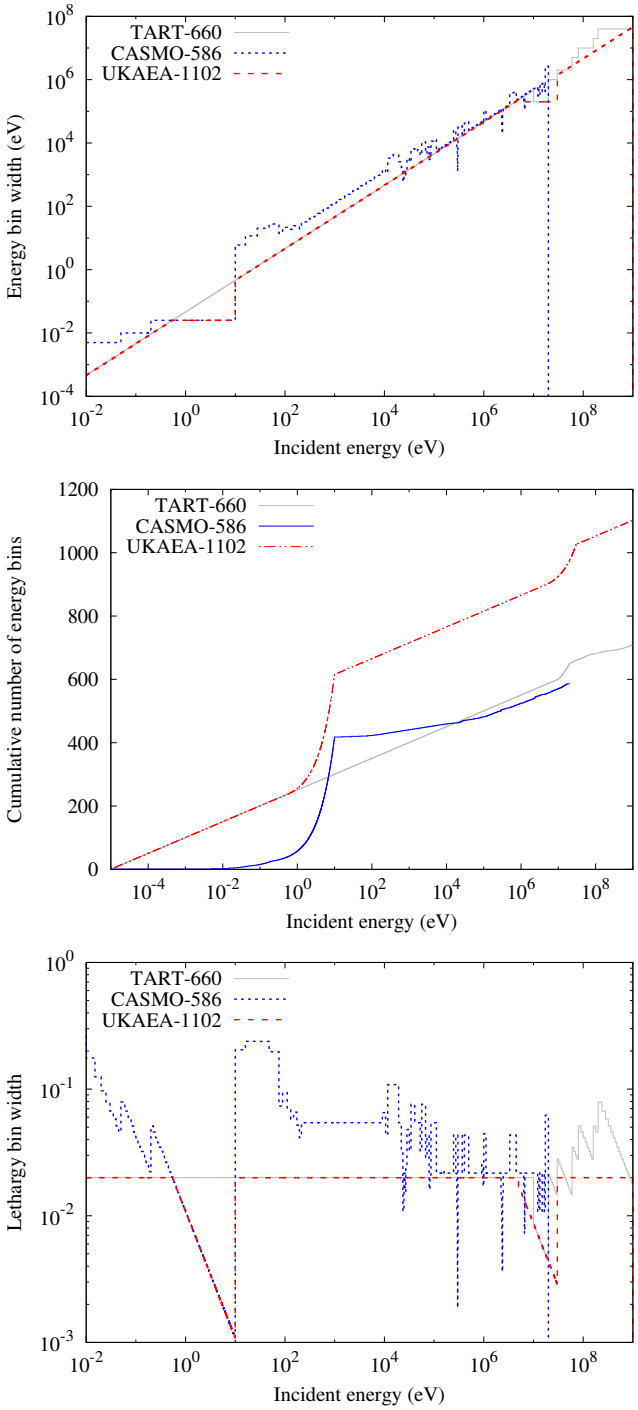

Fig. 3. Energy group structure for the TART-660, CASMO-586 and UKAEA-1102 group structures. Plots showing the energy bin width (top), cumulative number of energy groups and lethargy bin width as a function of incident particle energy (bottom).

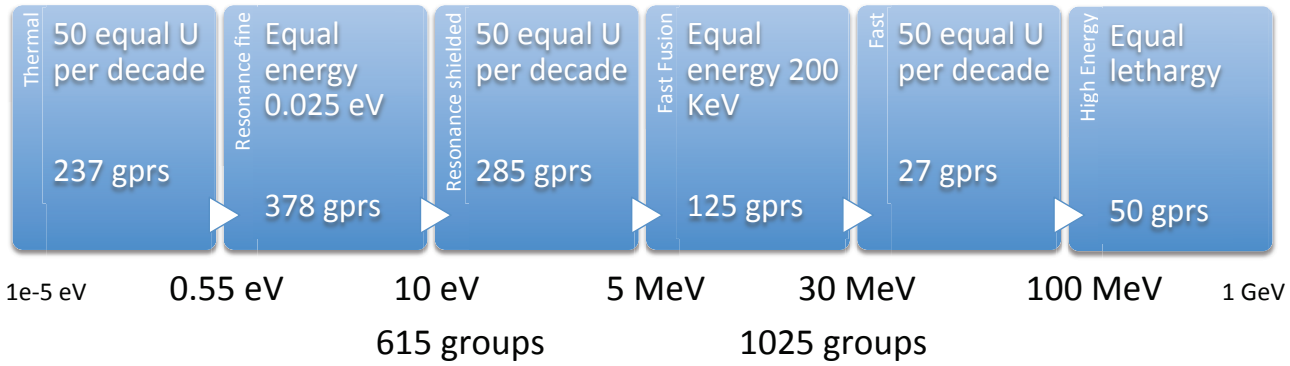

Fig. 4. UKAEA-1102 group structure description.

cross sections are computed by applying the self-shielding factors SSF to produce the effective cross sections. The effective SSF for the collapsed cross section is given by

$$ssf(p,y) = \frac{\sigma^{new}(p,y)}{\sigma^{LIB}(p,y)}. \tag{18}$$

The self-shielding factors may be applied wherever probability table data is provided and can be used to correct specific sets of reaction rates for desired nuclides, for example the energy-dependent self-shielding factors applied to the ^{238}U neutron capture in a typical PWR spectrum and fresh fuel composition, which is shown in Fig. 7. These can be automatically updated during irradiation, accommodating changes in both nuclide inventory and spectra to alter the dilutions and reaction rates, respectively.

1. Fission assembly simulations

As part of an international collaboration on uncertainty methods in reactor simulations [19], a set of reactor assemblies were modelled using CASMO-5 [15] with ENDF/B-VII.1 nuclear data. The neutron spectra for each fuel pin and volumetric power normalisation for some 50 steps of a 40 GWd/THM irradiation scenario were calculated by CASMO-5, providing the necessary input for FISPACT-II to follow the full inventory.

To accurately incorporate this data, consistent 586-group cross sections and probability tables were generated from and for ENDF/B-VII.1, including total energy-dependent kerma. The energy- and time-dependent self-shielding factors for each of the major reaction channels were employed, including fission and absorption for all actinides (see Fig. 7 and Fig. 1). ENDF/B-VII.1 independent fission yields for all available files and complete decay processes for all fission products were used in the simulation. To match the power normalisation of CASMO, the total reaction kerma for the full inventory was used to set a time-dependent neutron flux which was renormalised on a 10 hour time-step in order to maintain the constant power normalisation.[1]

[1]Since FISPACT-II has been designed to treat flux as constant during any time-step, this re-normalisation period was required to prevent the time-dependence of the flux from affecting the power normalisation.

One of the assemblies simulated, from Takahama-3 [20], has a lattice depiction in Fig. 5, including an array of burnable gadolinium poison rods and water-filled guide tubes. Average spectra for each pin, with material-specific probability table SSF's, were used to follow the inventory and compare directly with the CASMO-5 predictions. The simulation results with FISPACT-II were notably in agreement with the CASMO predictions, with ^{235}U concentration within 2% and ^{238}U within 0.5% at 45 GWd/THM burn-up, as shown in Figure 6. Similar agreement was found with the other assembly simulations of that collaboration [19].

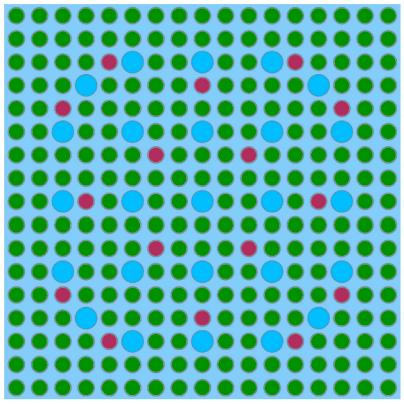

Fig. 5. Takahama-3 assembly lattice with standard fuel rods (green), gadolinium rods (pink) and guide tubes (blue), as depicted by CASMO-5.

2. Fusion material simulations

To illustrate the importance of having a group structure with sufficient resolution, we consider the example of tungsten [21, 22]. A sample of tungsten was irradiated at the high flux reactor HFR in Petten under the exercise EXTREMAT-II in

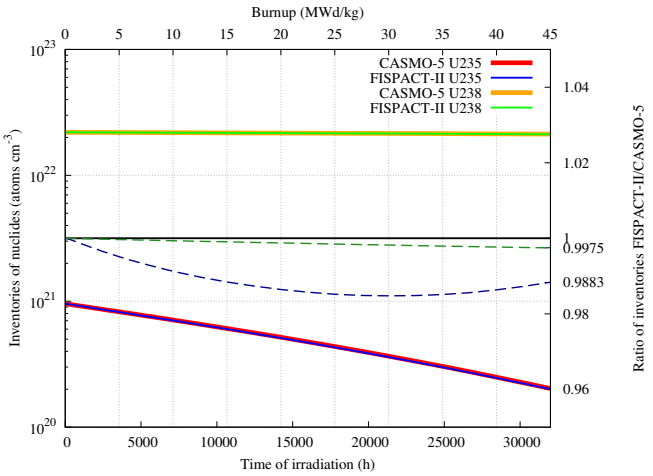

Fig. 6. Takahama-3 assembly uranium inventories from CASMO-5 and FISPACT-II simulations over a 45 GWd/THM simulation. The ratio of ^{235}U (ending at 1.2% difference) and ^{238}U (ending at 0.25% difference) are also shown.

2008-2009 for 8 cycles and at two different positions. The sample was positioned next to another experiment with very strong thermal neutron absorption properties. This occasioned the W sample to be exposed to a lower than normal (for HFR) fraction of thermal neutrons. The spectral shifts occasioned are depicted in Fig. 9 were the local C3 and C7 position thermal Maxwellian can be seen to be less prominent than in the typical (original) spectrum predicted for the sample locations in HFR.

The simulated HFR neutron flux profiles are represented in the fine 1102 structure and this allows the collapsed reaction rates to properly account for the spectral shifts and self-shielding effect that would otherwise not have been considered important or been noticed.

It is noticeable that in the case of the ^{186}W capture reactions (see Fig. 10 and 11) almost 50% of the RR comes from neutrons of energy below 10 eV, while for the ^{184}W capture (see Fig. 12) this 50% "threshold" is below 100 or 200 eV, depending on the HFR spectrum considered is the original or location-specific.

It is too often forgotten that the reaction rate is a full collapse of the energy-dependent cross section and incident flux that may on occasion emphasise the 1/E, thermal, giant resonances or other energy region – often shifting the region of importance between different targets, channels, spatial regions, etc. The energy-dependent cross sections for the ^{235}U fission and ^{238}U capture, as shown in Fig. 8, demonstrate this essential feature. In this case, the CASMO-586 group structure has been used with FISPACT-II for a Three Mile Island (TMI unit 1) spectrum, showing the fine resonance treatment below 10 eV with a less satisfying, coarse treatment for the lower tail of the thermal Maxwellian including the single group to 10^{-5} eV.

Without taking many thousands of ultra fine groups, it will always be impossible to fully capture all of the resolved resonances within all reaction channels of importance for any

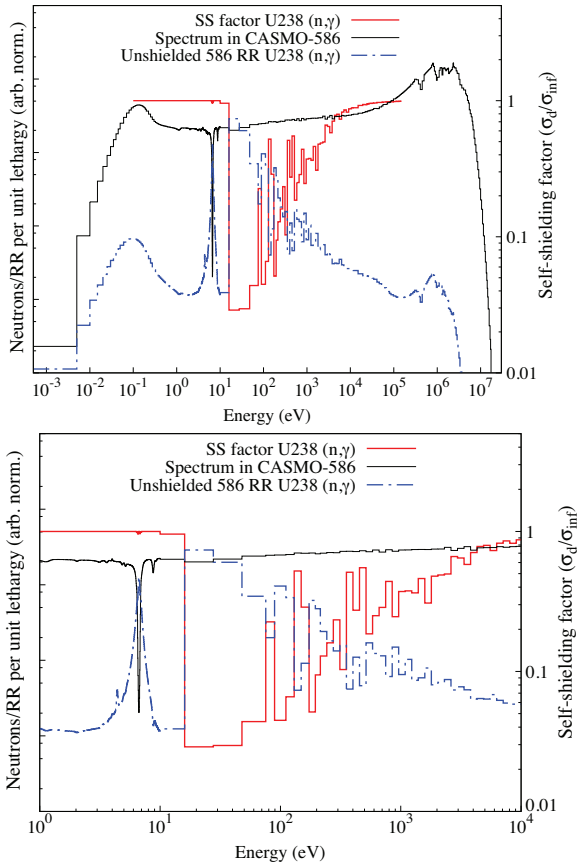

Fig. 7. Neutron spectrum, the unshielded ^{238}U(n, γ) cross section and the energy-dependent probability table self-shielding factors calculated for the fresh fuel composition in FISPACT-II using ENDF/B-VII.1. Global and zoomed-in plots are provided. The integrated self-shielding factor for this cross section is 0.18.

arbitrary application. While the UKAEA-1102 group follows the CASMO-586 treatment for giant resonances below 10 eV[2], the energies above 10 eV will often contribute non-negligibly to reaction rates, for example in the case of ^{238}U – even with the giant resonance resolved by a fine group. To solve this issue a self-shielding method must be employed which takes into account the dilution-specific aspects which are unique for any given material composition/region/reactor type. This is handled by the CALENDF-generated probability table self-shielding corrections within FISPACT-II, producing energy-dependent self-shielding for all resonant reaction channels, as can be seen in the ^{238}U capture of Fig. 7. These can be calculated throughout the simulation of, say, a burn-up of fission fuel, updating for the change in fuel composition over all fissile, time-dependent dilutions and full energy-spectrum.

The calculation of the reaction rates using the group-wise approach introduces unnecessary and often very significant

[2]For CASMO, this largely takes care of the ^{238}U capture self-shielding, while for general applications this solves the self-shielding issues for a great many more non-threshold reaction channels.

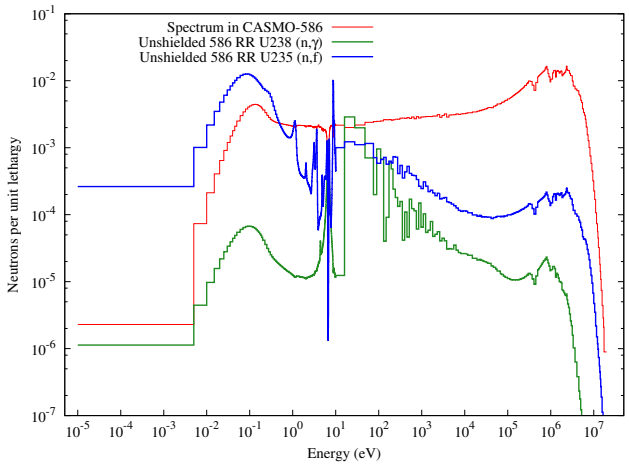

Fig. 8. Energy-dependent ^{235}U fission and ^{238}U capture reaction rates for a typical PWR flux.

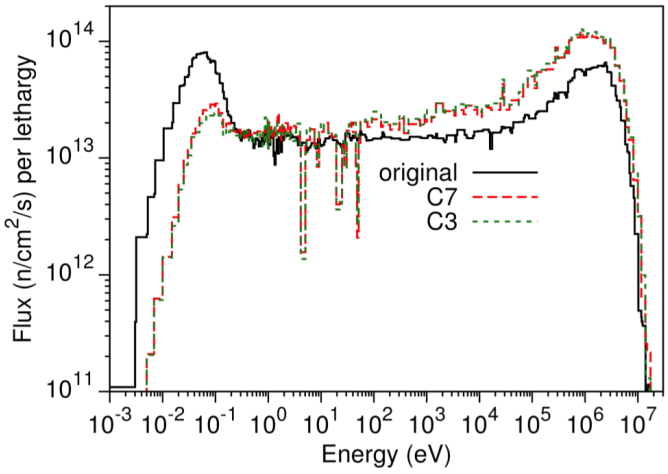

Fig. 9. HFR Petten spectra.

errors when and if

- the neutron flux grid is too coarse;
- the simulation does not account for the local heterogeneity and effects on spectra;
- the giant resonance region is not properly represented.

Other simulations directly benefit from this new modelling capabilities, including fusion materials technologies, beam-target physics, isotope production and transmutation aspects. Reactor physics may also benefit, particularly on the time-evolution of cladding and in-core non-fissile materials.

VI. CONCLUSIONS

For decades now, enhanced nuclear data forms such as probability tables have benefited most Monte Carlo and deterministic transport Boltzmann equation solvers. Now those same data forms are also able to benefit general-purpose time-dependent inventory Batemann solvers and which handle reac-

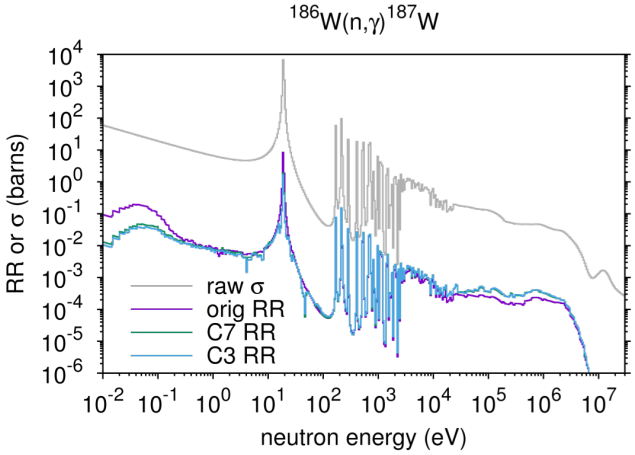

Fig. 10. HFR Petten ^{186}W cross sections and reactions rates.

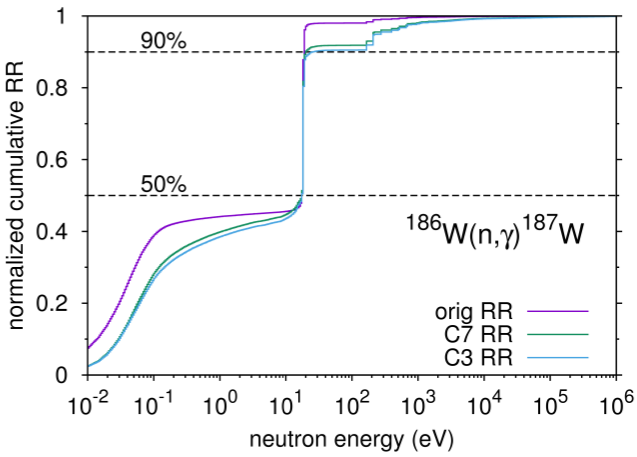

Fig. 11. HFR Petten ^{186}W normalised reactions rates.

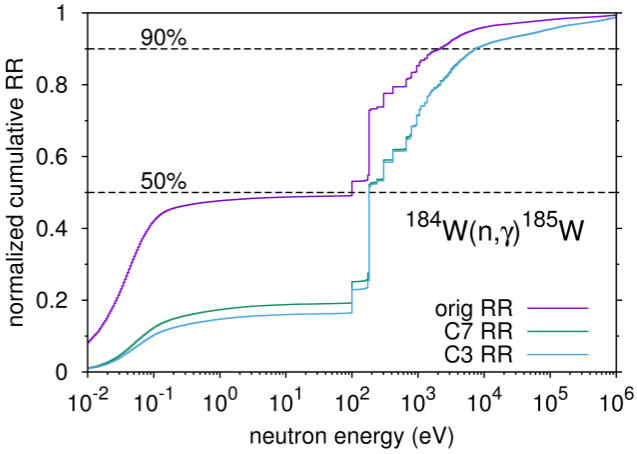

Fig. 12. HFR Petten ^{184}W normalised reactions rates.

tion data for all applications from fuel analysis to activation-transmutation studies.

The probability tables produced by CALENDF are now part of the multi-physics enhanced nuclear data forms accessible to the inventory code FISPACT-II. They offer adaptable self-shielding simulation capabilities for any reaction channels, isotopic composition of materials, reactor types and irradiation scenarios, fully propagating their impact on the reactions rates through general-purpose time-dependent simulations.

VII. ACKNOWLEDGMENTS

This work was funded by the RCUK Energy Programme under grant EP/1501045. To obtain further information on the data and models underlying this paper please contact PublicationsManager@ukaea.uk

REFERENCES

1. J.-CH. SUBLET, P. RIBON, and M. COSTE-DELCLAUX, "CALENDF-2010: User Manual," Tech. Rep. CEA-R-6277, ISSN 0429-3460, CEA (2011).
2. J.-CH. SUBLET and P. RIBON, "A Probability Table Based Cross Section Processing System: CALENDF - 2001," *J. Nuc. Sci. Tech.*, **39, Sup. 2**, 856–859 (2002).
3. J.-CH. SUBLET, J. EASTWOOD, J. MORGAN, M. GILBERT, M. FLEMING, and W. ARTER, "FISPACT-II: An Advanced Simulation System for Activation, Transmutation and Material Modelling," *Nuclear Data Sheets*, **139**, 77–137 (2017), special Issue on Nuclear Reaction Data.
4. J.-CH. SUBLET, J. EASTWOOD, J. MORGAN, M. FLEMING, and M. GILBERT, "FISPACT-II User Manual," Tech. Rep. UKAEA-R(11)11 Issue 8, UKAEA (Dec. 2016), see http://fispact.ukaea.uk.
5. J.-CH. SUBLET, R. BLOMQUIST, S. GOLUOGLU, and R. MAC FARLANE, "Unresolved resonance range cross section probability and self shielding factors," Tech. Rep. CEA-R-6227, ISSN 0429-3460, CEA (2009).
6. D. ROCHMAN, A. J. KONING, J. KOPECKY, J.-CH. SUBLET, P. RIBON, and M. MOXON, "From average parameters to statistical resolved resonances," *Annals of Nuclear Energy*, **51**, 60–68 (2013).
7. C. JOUANNE and J.-CH. SUBLET, "TRIPOLI-4.4 JEFF-3.1 Based Libraries," Tech. Rep. CEA-R-6125, ISSN 0429-3460, CEA (2006).
8. J.-CH. SUBLET, "JEFF-3.1, ENDF/B-VII and JENDL-3.3 Critical Assemblies Benchmarking With the Monte Carlo Code TRIPOLI," *IEEE Transactions on Nuclear Science*, **55**, *1*, 604–613 (Feb 2008).
9. J. M. RUGGIERI ET AL, "ERANOS 2.1:International Code System for GEN IV Fast Reactor Analysis," *International Congress on Advances in Nuclear Power Plants (ICAPP 2006)* (2006).
10. J.-CH. SUBLET, C. DEAN, and D. PLISSON-RIEUNIER, "ECCOLIB-JEFF-3.1 Based Libraries," Tech. Rep. CEA-R-6100, ISSN 0429-3460, CEA (2006).
11. I. BONDARENKO, editor, *Group Constants for Nuclear Reactor Calculations*, Consultant Bureau, New York (1964).
12. G. BELL and S. GLASSTONE, *Nuclear Reactor Theory*, Van Nostrand Reinhold, New York (1970).
13. V. GOPALAKRISHNAN and S. GANESAN, "Self-Shielding and Energy Dependence of Dilution Cross-Section in the Resolved Resonance Region," *Ann. Nucl. Energy*, **25**, *11*, 839–857 (1998).
14. R. MACFARLANE, R. BLOMQUIST, D. CULLEN, and J.-CH. SUBLET, "A Code Comparison Study for the Bitten Critical Assembly," Tech. Rep. LA-UR-08-4668, LANL (2008).
15. J. RHODES, K. SMITH, and D. LEE, "CASMO-5 Development and Application," in "proceedings PHYSOR-2006, Advances in Nuclear Analysis and Simulation," American Nuclear Society, Vancouver, BC, Canada (September 2006).
16. D. CULLEN, "PREPRO-2015, 2015 ENDF-6 Preprocessing codes," Tech. Rep. IAEA-NDS-39 (Rev. 16), IAEA (2015).
17. A. HODGSON, R. GRIMES, M. RUSHTON, and O. MASDEN, "The Impact of Neutron Cross Section Group Structures on the Accuracy of Radiological Source Models," *Nuclear Science and Engineering*, **181**, *3*, 1–8 (2015).
18. M. FLEMING, L. MORGAN, and E. SHWAGERAUS, "Optimisation Algorithms for Multi-Group Energy Structures," *Nuclear Science and Engineering*, **183**, *2*, 179–184 (June 2016).
19. D. ROCHMAN, O. LERAY, M. HURSIN, H. FERROUKHI, A. VASILIEV, A. AURES, F. BOSTELMANN, W. ZWERMANN, O. CABELLOS, C. DIEZ, J. DYRDA, N. GARCIA-HERRANZ, E. CASTRO, S. VAN DER MARCK, H. SJÖSTRAND, A. HERNANDEZ, M. FLEMING, J.-CH. SUBLET, and L. FIORITO, "Nuclear Data Uncertainties for Typical {LWR} Fuel Assemblies and a Simple Reactor Core," *Nuclear Data Sheets*, **139**, 1–76 (2017), special Issue on Nuclear Reaction Data.
20. C. SANDERS and L. GAULD, "Isotopic analysis of high-burnup PWR spent fuel samples from the Takahama-3 reactor," Tech. Rep. NUREG/CR-6798, ORNL/TM-2001/259, Oak Ridge National Laboratory (2003).
21. J.-CH. SUBLET and M. SAWAN, "Self-shielding effects in a tungsten layer in a fusion device," *Fusion Engineering and Design*, **45**, *1*, 65 – 73 (1999).
22. M. R. GILBERT and J.-CH. SUBLET, "Neutron-induced transmutation effects in W and W-alloys in a fusion environment," *Nucl. Fus.*, **51**, 043005 (2011).